See also N. Kristianpoller and M. Israeli, Phys. Rev. B 2, 2175 (1970).
[16]R. C. Linares, J. Opt. Soc. Am. 56, 1700 (1966).
[17]A. K. Trofimov, Izv. Akad. Nauk. S. S. S. R., Ser. Fiz. 25, 460 (1961).
[18]M. J. Weber, Phys. Rev. 171, 283 (1968).
[19]J. L. Merz and P. S. Pershan, Phys. Rev. 162, 217 (1967).
[20]J. L. Bates, AEC Report No. BNWL-457, 1957 (unpublished).
[21]M. H. L. Price, Proc. Phys. Soc. (London) A63, 25 (1950).
[22]M. H. L. Price, Nuovo Cimento Suppl. 6, 817 (1957).
[23]T. G. Castner and W. Kanzig, J. Phys. Chem. Solids 3, 178 (1957).
[24]S. A. Al'tshuler and B. M. Kozyrev, *Electron Paramagnetic Resonance* (Academic, New York, 1964), Secs. 3.3 and 6.5.
[25]C. P. Slichter, *Principles of Magnetic Resonance* (Harper and Row, New York, 1963), Secs. 7.2 and 7.4.
[26]W. Low and D. Shaltiel, J. Phys. Chem. Solids 6, 315 (1958).
[27]M. Abraham, R. A. Weeks, G. W. Clark, and C. B. Finch, Phys. Rev. 137, A138 (1965).
[28]M. M. Abraham, E. J. Lee, and R. A. Weeks, J. Phys. Chem. Solids 26, 1249 (1965).
[29]V. I. Neeley, J. B. Greber, and W. J. Gray, Phys. Rev. 158, 809 (1967).
[30]M. M. Abraham, C. B. Finch, R. W. Reynolds, and H. Zeldes, Phys. Rev. 187, 451 (1969).
[31]J. L. Kolopus, C. B. Finch, and M. M. Abraham, Phys. Rev. B 2, 2040 (1970).
[32]W. E. Danforth, *Advances in Electronics*, Vol. 5 (Academic, New York, 1953).
[33]L. Pincherle, Proc. Phys. Soc. (London) A64, 648 (1951).
[34]B. S. Gourary and F. S. Adrian, Phys. Rev. 105, 215 (1957).
[35]B. S. Gourary and F. S. Adrian, *Solid State Physics*, Vol. 10 (Academic, New York, 1960).
[36]A. H. Kahn and C. Kittel, Phys. Rev. 89, 315 (1953).
[37]W. E. Blumberg and T. P. Das, Phys. Rev. 110, 647 (1958).
[38]F. S. Ham, Phys. Rev. 166, 307 (1968).

PHYSICAL REVIEW B VOLUME 4, NUMBER 8 15 OCTOBER 1971

Direct Observation of Isolated $J=1$ Pairs in Solid Deuterium and Hydrogen by Raman Scattering

Isaac F. Silvera* and Walter N. Hardy†
North American Rockwell Science Center, Thousand Oaks, California 91360

and

John P. McTague
Department of Chemistry, University of California,‡ Los Angeles, California 90024

(Received 1 March 1971)

Spectra due to the orientational states of isolated $J=1$ impurity pairs in solid hydrogen and deuterium have been observed by Raman scattering in the wave-number range 2.3–7 cm^{-1}. The results give a direct measure of the pair energy levels and can be used to determine the anisotropic pair interactions. To within experimental accuracy, no deviation from the dominant electric quadrupole-quadrupole interaction was observed. Expressions are developed for the scattering efficiency which agree well with experiment. Zero-point-motion averages of the interactions are calculated using several quantum crystal wave functions and a comparison is made with the measured frequencies. The collective wave functions give better agreement with experiment than the Hartree single-particle wave functions.

I. INTRODUCTION

The solid hydrogens (hydrogen, hydrogen deuteride, and deuterium) are the simplest molecular solids and present unique opportunities for the study of intermolecular interactions in the crystalline state. Their interactions with electromagnetic radiation provide rich spectra that can be interpreted in terms of intermolecular forces; the variation of mass by a factor of 2 with little change in the electronic structure enables studies of mass effects; and the anisotropic interactions can be isolated by studying appropriate mixtures of the ortho-para species. In the condensed phase the hydrogens, as distinct from most solids, exhibit well-resolved rotational spectra. This is a consequence of the fact that the free-molecule rotational energy spacings are much larger than the anisotropic potentials in the solid, and thus the rotational quantum number J remains a good quantum number.

At the low temperatures of the solid (< 20 K) essentially all hydrogen (deuterium) molecules are in the lowest accessible rotational level, namely, $J=0$ for para-hydrogen (p-H_2) and ortho-deuterium (o-D_2), and $J=1$ for ortho-hydrogen (o-H_2) and para-deuterium (p-D_2). For low concentrations of $J=1$ molecules the lattice structure is hexagonal close packed (hcp). Molecules in the $J=0$ state interact only isotropically, while isolated $J=1$ molecules experience very weak anisotropic interac-

tions (≈ 0.01 cm^{-1}) due to crystalline fields.[1] At the other extreme, namely, a lattice of $J=1$ molecules, there is an order-disorder phase transition driven by the anisotropic intermolecular interactions in which the structure changes from hcp to fcc and the molecular axes assume preferential orientations with respect to the crystalline axes.[2] Although the part of the energy spectrum due to the collective librational states in the ordered phase[3,4] is determined by the anisotropic potential, the form of the anisotropic interaction is best studied via the spectrum of isolated pairs of $J=1$ molecules in a $J=0$ lattice.

The dominant part of the anisotropic pair potential is the molecular electric-quadrupole-quadrupole (EQQ) interaction, and this partially lifts the ninefold degeneracy of the pair levels. Splittings of the pair energy levels have been obtained previously by a number of indirect techniques; however, these measurements are mainly sensitive to the lowest-excited-pair levels and there has been a scatter of reported values for Γ, the EQQ coupling parameter. Infrared spectroscopic techniques have been used to observe sidebands of molecular vibrational transitions in solid H_2 and these were subsequently identified as a combination mode involving the lowest-pair orientational levels.[5] Inelastic-neutron-scattering linewidths[6] of the $J=0\rightarrow 1$ transitions in H_2 have been related to the EQQ interaction. Thermodynamic measurements such as specific heat[7] and $(\partial P/\partial T)_V$[8] as well as the temperature dependence of the NMR lines for $J=1$ pairs[9] have also been used to determine Γ. The only reported value of Γ for p-D_2 pairs has been obtained from measurements of $(\partial P/\partial T)_V$ and is substantially different from that given here.[8] None of the techniques used previously are sensitive to deviations of the anisotropic interactions from EQQ.

We have made direct observations of the pure orientational transitions of pairs of $J=1$ deuterium and hydrogen molecules imbedded in a $J=0$ host lattice. These measurements provide detailed information concerning the form of the anisotropic pair potential; to within experimental error no deviation from the dominant EQQ interaction was observed. Large, previously noted,[10] reductions of the experimentally determined value of Γ from that expected for a rigid lattice of molecules are confirmed. We have calculated the renormalization of Γ due to zero-point motion of the lattice using several forms of quantum crystal wave functions. The collective self-consistent wave functions of Klein and Koehler[11] give better agreement with experiment than previous results using single-particle-type wave functions.

II. ANISOTROPIC INTERMOLECULAR INTERACTIONS

A quantitative treatment of the anisotropic intermolecular interactions in solid hydrogen was given by Nakamura[12] in 1955. He estimated the magnitude of the anisotropic potential terms in the rigid lattice approximation (no zero-point motion) for a pair of $J=1$ molecules and showed that the EQQ term is the dominant anisotropic pair interaction. Harris[10] has refined the calculation of the pair spectrum taking into account effects of zero-point motion, non-EQQ anisotropic pair interactions, crystal-field effects arising from the lowering of the site symmetry of the molecules whose neighbors are other than $J=0$, and dielectric effects due to the interactions of the pairs with dipole and quadrupole moments which they induce in the surrounding molecules.

A schematic representation of the energy-level diagram for the $J=1$ pairs is shown in Fig. 1 for a general anisotropic pair interaction. The eigenstates are numbered from 1 to 9 for ease of reference and then expressed in terms of total pair rotational angular momentum F and its projection on the intermolecular axis M_F and also in terms of the individual angular momentum projections m_i. The general intermolecular potential[10] expanded in terms of the spherical harmonics is given within the $J=0$ and $J=1$ manifold of states by

$$V = A(R) + (16\pi/5)^{1/2} B(R)[Y_2^0(\Omega_1) + Y_2^0(\Omega_2)] + 4\pi \sum_{j\mu} \epsilon_j(R)\alpha_j C(22j;\ \mu, -\mu) Y_2^{\mu}(\Omega_1) Y_2^{-\mu}(\Omega_2), \tag{1}$$

where Ω_1 and Ω_2 specify the angles of the molecular axes with respect to the vector $\vec{R}$ connecting the molecular centers, and $C(L_1L_2L_3;\ M_1, M_2)$ is a Clebsch-Gordan coefficient.[13] The term $A(R)$ represents the isotropic pair interaction and $B(R)$ the potential involving the orientation of a single molecule. The coefficients $\epsilon_j\alpha_j$ vanish for odd j with $\alpha_0=\sqrt{5}$, $\alpha_2=\sqrt{\frac{7}{2}}$, and $\alpha_4=\sqrt{70}$. A pure EQQ potential corresponds to $\epsilon_4=\frac{5}{6}\sqrt{(70)}\Gamma$ with the coupling parameter $\Gamma=\frac{6}{25}e^2Q^2/R^5$. Here eQ is the molecular electric quadrupole moment and R the intermolecular separation. The dominant EQQ interaction lifts the ninefold pair degeneracy, yielding four distinct levels of maximum splitting 10Γ. The rigid lattice value $\Gamma=\Gamma_0$, evaluated with R at R_0, the equilibrium nearest-neighbor separation in the solid, is 0.839 cm^{-1} for D_2 and 0.698 cm^{-1} for H_2,[10] resulting in transition frequencies in the range 1–8 cm^{-1}. ("Frequency" here is measured in wave-number units cm^{-1}.)

The major perturbation of the spectrum is due to the large zero-point motion of the lattice (see Sec. V). The dominant effect of the zero-point motion is to renormalize the EQQ interaction, and can be represented by scaling down Γ by 10 to 30% (see Sec. V). A smaller effect arises from the rotational-phonon coupling, and increases the effective pair interaction by 5 to 10%.

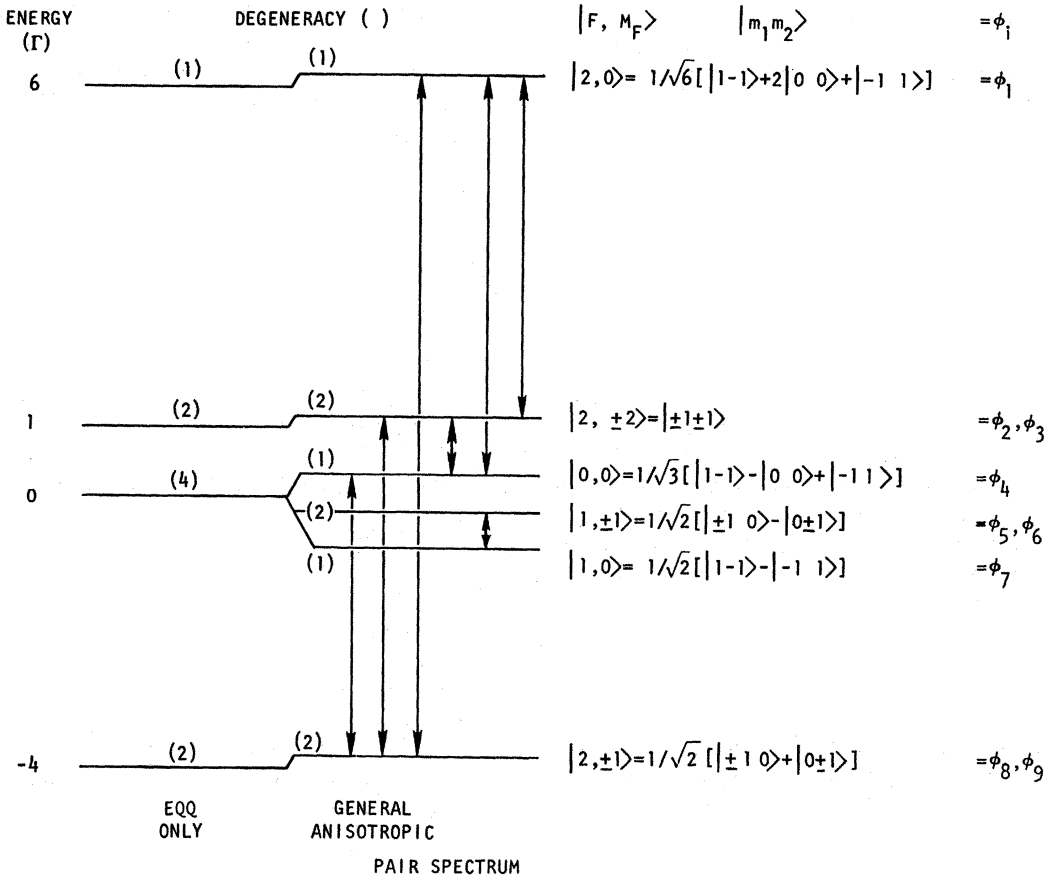

FIG. 1. $J=1$ pair energy levels. The eigenstates are given in terms of the total pair rotational angular momentum F and its projection on the intermolecular axis M_F, and also in terms of the individual molecular angular momentum projections m_i. For convenience, the states are also numbered 1–9 (the lower numbered degenerate states correspond to the upper signs). Raman active transitions are indicated by arrows. The non-EQQ splittings are unknown and are shown only schematically.

The non-EQQ part of the anisotropic pair potential (including the crystal-field term arising from the lowering of the site symmetry of a molecule whose neighbors are other than $J=0$[14]) has been shown by Harris to further lift the degeneracy of the pair levels as shown schematically in Fig. 1. These potential parameters are not well known, but have been estimated to be <0.1 cm^{-1}. Finally, the dielectric interactions not only shift the center of gravity of the pair levels but can also remove the remaining degeneracies. Theoretical estimates of the frequencies of the observed transitions are given in Table I.

III. EXPERIMENTAL

Direct observation of transition frequencies in the 1–10-cm^{-1} spectral region represents a difficult task for either absorption or Raman spectroscopy. In the former technique the difficulties are due mainly to the lack of a conveniently tunable high-power source. In the Raman technique the problem that arises for small frequency shifts is the separation of the weak Raman signal from the unshifted scattered laser light which may be of order 10^4–10^6 times stronger, and whose apparent width corresponds to the spectrometer slit function. The problem is particularly severe for solids since light can be scattered by cracks, imperfections, etc.

Using a gaseous iodine filter we have been able to observe several of the Raman active transitions of nearest-neighbor pairs of $J=1$ o-H_2 and p-D_2 in host lattices of $J=0$ p-H_2 and o-D_2, respectively. Right angle scattering was observed in the temperature range $1.16 \leq T \leq 4.2$ K in samples which were apparently single crystal of size ~ 1 cm^3. The growth techniques have been described previously.[3,15] Samples were prepared by mixing known amounts of normal $D_2(H_2)$ with high purity o-D_2 (p-H_2). Concentration levels of the $J=1$ molecules were confirmed by relative intensity measurements of the $J=0\rightarrow 2$ and $J=1\rightarrow 3$ rotational Raman lines in the

solid phase. In the D_2 sample an HD impurity concentration of 1% was present, as determined by the intensity of its $J=0\rightarrow 2$ transition.

Raman transitions were excited by the 5145-Å line of a Coherent Radiation Laboratories Model 52 argon ion laser. The lower-frequency (<5 cm^{-1}) Raman lines would normally be obscured at the laser frequency by the intense scattering caused by crystal surfaces, imperfections, etc. This signal can be reduced by factors of 10^3–10^4 with an ingenious scheme devised by Chase, Davis, Devlin, and Geschwind.[16] Iodine gas has two electronic-vibrational-rotational absorption lines of significant strength that fall within the gain profile of the 5145-Å lasing line. By operating the laser on a single mode at the same frequency as one of the I_2 rotational lines, a cell of I_2 gas can be used as a very high Q filter to absorb the unshifted laser light. Such a cell was mounted between the scattering region and the monochromator, enabling useful spectra to be recorded down to frequency shifts of ~ 2.3 cm^{-1}. The use of the filter reduced the signal by approximately 10, of which a factor 2 was due to laser power reduction when single moded and the rest was due to cell losses. Severe difficulties were encountered in the operation of the filter owing to the tendency of the laser to mode hop, which destroys the frequency overlap with the I_2 line. As a consequence, the filter efficiency was continuously monitored as the spectra were taken in order to identify spurious peaks from laser mode hopping. The monitor signal was obtained by passing a small percent of the laser light through transverse windows in the I_2 cell and displaying the photodiode detected signal simultaneously with the Raman signal as shown in Fig. 2. Since instabilities generally occurred every few minutes, scan rates and integration times were short, leaving something to be desired in the recorded signal-to-noise ratio. Under these conditions, *several scans were always made through important features of the spectra in order to increase our confidence levels in the identification.* Frequencies could be measured to an accuracy better than 0.1 cm^{-1} using a frequency calibrator previously described.[3,17]

In Fig. 3 are shown the observed pair spectra for samples of 2.7% p-D_2 in o-D_2 and 2% o-H_2 in p-H_2, corresponding to pair concentrations of 0.27% and 0.17%, respectively, for random $J=1$ distributions.[18,19] These spectra, which exhibit two features, are *representative of several scans.* The higher-frequency lines are of lower intensity and were observed without the iodine cell in order to take advantage of the increased system throughput. Use of the iodine cell allowed the inner line to be clearly observed in the D_2 sample, whereas in H_2 this line was only partially resolved from the unshifted laser component, preventing a peak frequency assignment. The shoulder of this peak is identified in Fig. 3. Frequencies are listed in Table I. The higher-frequency features are identified as the $|2,\pm1\rangle\rightarrow|2,0\rangle$ transitions of energy $\nu_h=10\Gamma$ (for EQQ interactions only). At $T=0$, features should occur at frequencies 4Γ and 5Γ, corresponding to the transitions $|2,\pm1\rangle\rightarrow|0,0\rangle$ and $|2,\pm1\rangle\rightarrow|2,\pm2\rangle$. However, the signal-to-noise ratio was inadequate to determine whether the observed feature near 3 cm^{-1} in D_2 was structured or not. We have therefore assumed that the frequency ν_l is the Raman intensity-weighted center of gravity of the active transitions:

$$\nu_l=\frac{\sum \nu_{ij}S_{ij}}{\sum S_{ij}}, \tag{2}$$

where ν_{ij} is the transition frequency from state i to j, and S_{ij} the scattering efficiency given in Sec. IV.

Transitions from thermally populated intermediate levels (see Fig. 1) to the highest level could not be identified due to inadequate signal-to-noise ratio. However, further confirmation of the identification of the pair levels was provided by the temperature and concentration dependence of their intensities. Figure 4 shows the $|2,\pm1\rangle\rightarrow|2,0\rangle$ transition for $T=4.2$ and 1.25 K, the relative intensities agreeing within signal-to-noise limitations

TABLE I. Experimental and theoretical pair frequencies. ν_h is the transition frequency from states 8 or 9 to 1, while ν_l is the Raman intensity weighted transition frequency defined in Eq. (2).

		EQQ theor freq.	Rigid lattice $\Gamma=\Gamma_0$ (cm^{-1})	Renormalized EQQ[a] $\Gamma=\xi_{54}\Gamma_0$ (cm^{-1})	Dielectric shift[a] $\Delta\nu$ (cm^{-1})	Resultant theor freq.[b] (cm^{-1})	Expt freq. (cm^{-1})	Non-EQQ estimate $\Delta\nu$ (cm^{-1})	Rot.-phonon interaction
D_2	ν_h	10Γ	8.39	6.65	−0.25	6.40	6.85±0.1	···	Increase in ν_h and ν_l of order 5 to 10%
	ν_l	4.43Γ	3.72	2.95	−0.12	2.83	2.98±0.2	···	
H_2	ν_h	10Γ	6.98	4.77	−0.12	4.65	5.51±0.1	−0.01	
	ν_l	4.43Γ	3.09	2.11	−0.06	2.05	≤2.45	+0.09	

[a]Interaction averaged with collective wave function.

[b]Non-EQQ and rotation-phonon contributions not included.

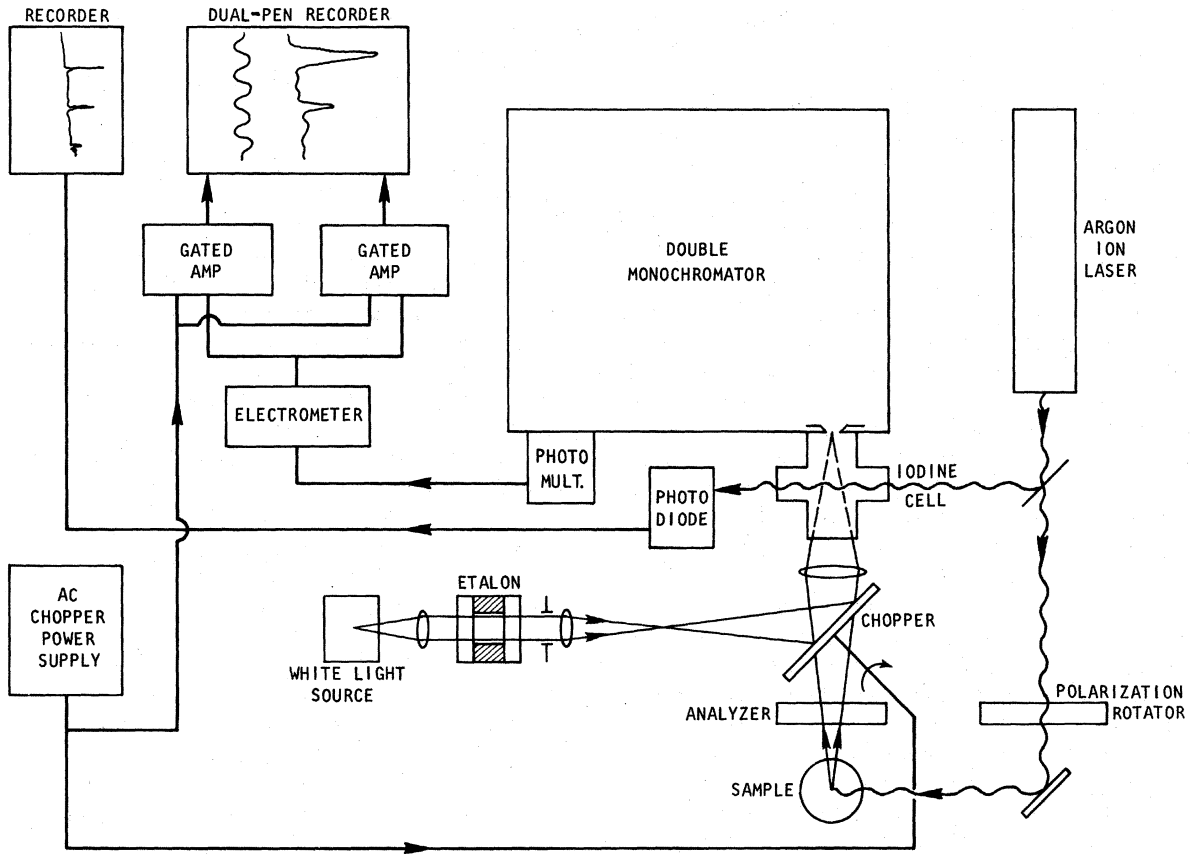

FIG. 2. Block diagram of the experimental scattering apparatus, showing the laser, sample, monochromator, iodine cell, and the Fabry-Perot fringe calibrator.

with the theoretical value of 2.2 for the ratios of the low-temperature to the high-temperature intensity. The intensities are about a factor of 20 lower than the weak optical-phonon line which is again about a factor of 500 weaker than the $J=0\rightarrow 2$ transitions.[20] Changing the concentration of $J=1$ species had the expected behavior. For concentrations less than ~1.5% the intensities were too low for useful spectra. If the concentrations were greater than ~4%, the lines were broadened to the extent that most of the increased intensity appeared in the wings of the lines which did not effectively increase the signal-to-noise ratio, and the contributions from isolated n-fold clusters ($n>2$) are difficult to separate. The optimum concentration was 2–3% $J=1$ species.

Relative intensities of the two features in D_2 were not obtained directly since the lines were observed with and without the I_2 filter. However, by comparing each line to the intensity of the $J=0\rightarrow 2$ transitions, the relative intensity of the low-frequency feature to the high-frequency feature was determined to be 10 ± 5.

IV. RAMAN INTENSITIES

In this section we calculate the Raman intensities for transitions between pair energy levels. In the polarizability approximation, the right angle Raman scattering efficiency for a transition from state Φ_i to Φ_j is given by[21]

$$S^{\sigma\rho}(i\rightarrow j)=\tfrac{1}{3}c_2(\omega/c)^4\rho_0 n_i \times\textstyle\sum_k |\langle j|\,\alpha^k_{\sigma\rho}\,|i\rangle|^2\,\delta(\omega_s-\omega_{ij})\,, \quad (3)$$

where $S^{\sigma\rho}_{ij}$ is the fraction of incident light scattered per unit frequency per unit solid angle per unit length of the crystal, and σ, ρ denote the polarizations of the incident and scattered light, respectively. The product of the pair mole fraction c_2 and the number of molecules/volume ρ_0 is the pair concentration; n_i is the thermal population factor of the state Φ_i, ω_s the frequency shift of the light, and ω_{ij} the frequency of the pair transition. The sum is over the twelve possible pairs as distinguished by their orientations relative to the crystal axes. $\alpha^k_{\sigma\rho}$ is the pair molecular polarizability expressed in the

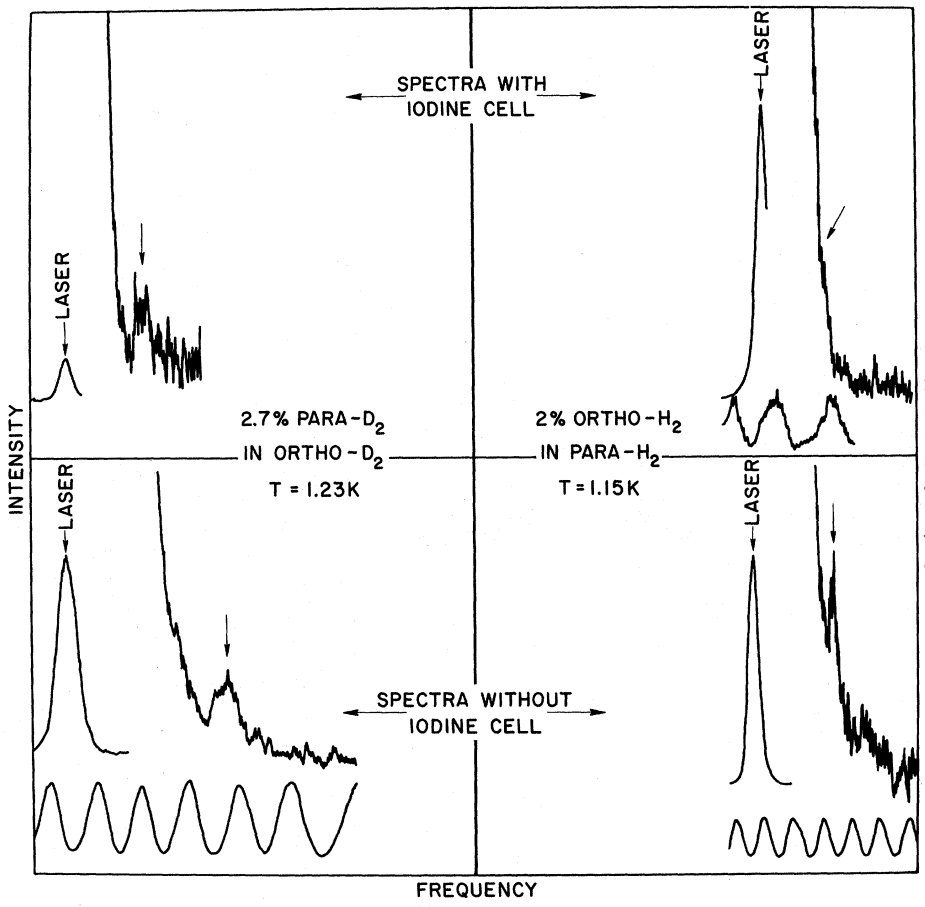

FIG. 3. Raman spectra of the pair transitions. A linear frequency axis could not be shown because of the nonlinearity of the spectrometer drive as indicated by the irregularity of fringe spacing which is a constant, 2.057 cm^{-1}. The width of the laser line is an indication of the instrumental resolution.

laboratory frame (σ, $p=X$, Y, or Z), where k indexes the twelve possible pair orientations in the hcp lattice. The principal task is to develop an expression for $\alpha_{\sigma\rho}^{k}$ and then evaluate this within the pair states. The selection rules can be seen immediately since the polarizability tensor is even and transforms as Y_2^m, which requires the matrix element of Eq. (2) to be nonzero only for $\Delta F=2, 0$.

The twelve tensors $\alpha_{\sigma\rho}^{k}$ are most easily found by determining $M^2=|\langle j|\,\alpha_{\sigma\rho}^{P}\,|i\rangle|^2$ for an arbitrary orientation of the pair P with respect to the laboratory frame and then evaluating it at the pair angles in the hcp lattice. The pair polarizability tensor is assumed to be the simple sum of the individual polarizabilities of the molecules 1 and 2:

$$\alpha_{\sigma\rho}^{P}=\alpha_{\sigma\rho}(\Omega_1)+\alpha_{\sigma\rho}(\Omega_2), \tag{4}$$

where Ω_1 and Ω_2 are the same as in Eq. (1) and are shown in Fig. 5. For a diatomic molecule, the Cartesian components of the anisotropic part of the polarizability tensor can be written as[22]

$$\alpha_{XY}(\Omega_i)=\frac{\beta}{4}\left(\frac{15}{2\pi}\right)^{1/2} i[Y_{2\text{-}2}(\Omega_i)-Y_{22}(\Omega_i)]\,,$$

$$\alpha_{XZ}(\Omega_i)=\frac{-\beta}{4}\left(\frac{15}{2\pi}\right)^{1/2}[Y_{2\text{-}1}(\Omega_i)-Y_{21}(\Omega_i)]\,,$$

$$\alpha_{YY}(\Omega_i)=\frac{-\beta}{4}\left(\frac{15}{2\pi}\right)^{1/2}[(\tfrac{2}{3})^{1/2}Y_{20}(\Omega_i)+Y_{22}(\Omega_i)+Y_{2\text{-}2}(\Omega_i)]\,, \tag{5}$$

$$\alpha_{YZ}(\Omega_i)=\frac{-\beta}{4}\left(\frac{15}{2\pi}\right)^{1/2} i[Y_{21}(\Omega_i)+Y_{2\text{-}1}(\Omega_i)]\,,$$

where $\beta=8\pi/15(\alpha_{\parallel}-\alpha_{\perp})$, $\alpha_{\parallel}$ and $\alpha_{\perp}$ are the principal values of the polarizability tensor for the hydrogen molecule, and Ω_i designates the orientation of the z_i axis in the pair fixed frame (see Fig. 5). The matrix elements required for Eq. (2) are then easily evaluated in terms of the $|m_1m_2\rangle$ representation given in Fig. 1.

The components of the polarizability tensor evaluated between the initial and final states, $\langle j|\alpha_{\sigma\rho}^{P}|i\rangle$, can be separated into three groups:

$$-\beta A_{ij}\begin{pmatrix}0 & 0 & \mp 1\\ 0 & 0 & i\\ \mp 1 & i & 0\end{pmatrix}, \tag{6}$$

where $A_{81}=A_{91}=\frac{1}{8}\sqrt{\frac{3}{2}}$, $A_{82}=A_{93}=\frac{9}{16}$, $A_{84}=A_{94}=-\sqrt{\frac{3}{16}}$,

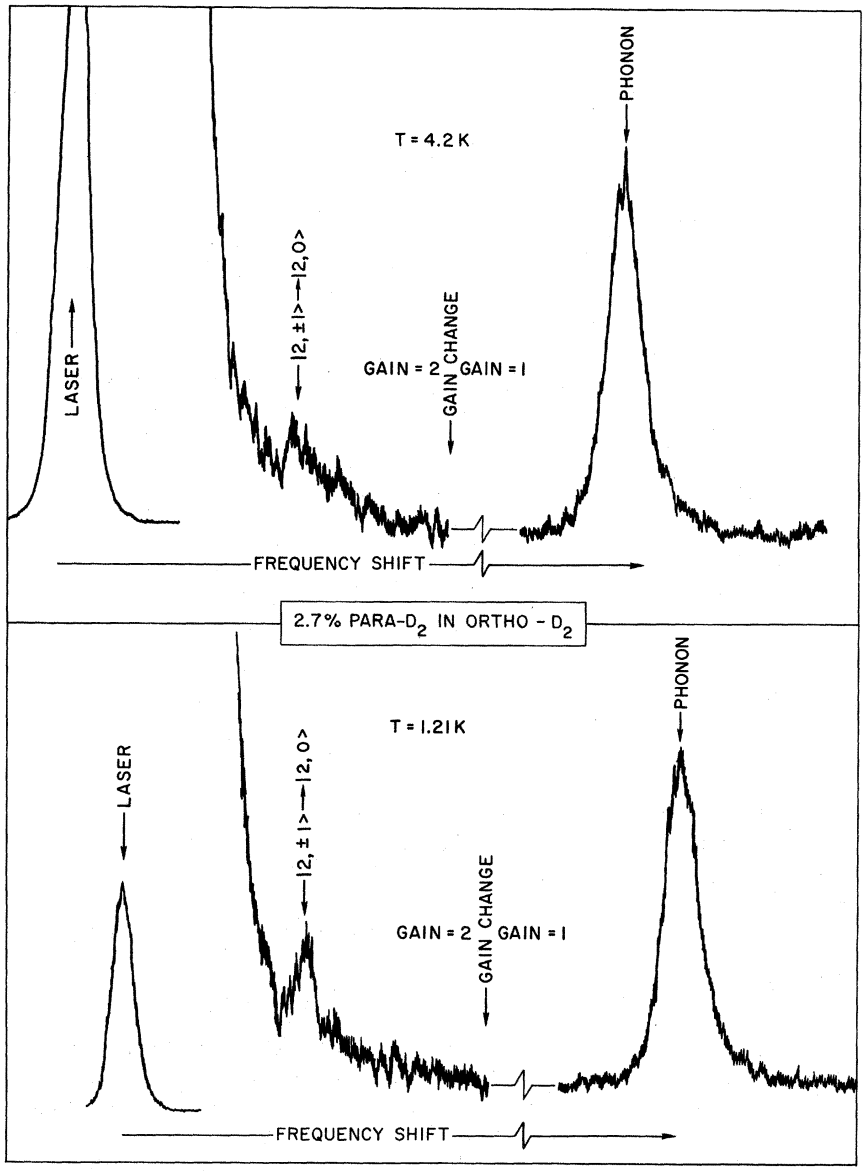

FIG. 4. Raman spectra in deuterium showing the effect of temperature on the intensity of one of the pair transitions. As a comparison of intensity, the "weak" optical-phonon line at 35.83 cm^{-1} is shown. The two frequency axes are not calibrated absolutely or relative to each other for these purposes of comparison.

$A_{75} = -A_{76} = -\frac{9}{16}\sqrt{2}$;

$$(\tfrac{2}{3})^{1/2}\beta A_{ij}\begin{pmatrix}1&0&0\\0&1&0\\0&0&-2\end{pmatrix}, \tag{7}$$

with $A_{41} = \sqrt{\frac{3}{4}}$; and

$$\beta A_{ij}\begin{pmatrix}1&\mp i&0\\\mp i&-1&0\\0&0&0\end{pmatrix}, \tag{8}$$

with $A_{42} = A_{43} = \sqrt{\frac{3}{4}}$, and $A_{31} = A_{21} = \frac{1}{4}\sqrt{\frac{3}{2}}$. For each pair of A_{ij} given, the first corresponds to the upper sign in the matrix. All other A_{ij} are zero. The tensors are complex because the degenerate pair states used are complex. They can be put in the usual real form by a suitable unitary transformation such that all of the states are real.

To find the total intensity for all pair orientations, we take the pair z axis to be at an arbitrary orientation designated by angles θ, Φ with respect to the laboratory scattering frame (whose Z axis also coincides with the crystal c axis to correspond with experiment) as in Fig. 5. The squared matrix elements in the scattering frame are then of the form[23]

$$|\langle j|\alpha_{XY}|i\rangle|^2 = \Big|\sum_{\sigma\rho} e_X^{\sigma}\langle m_1 m_2|\alpha_{\sigma\rho}^{P}|m_1' m_2'\rangle e_Y^{\rho}\Big|^2, \text{ etc.}, \tag{9}$$

where e_X^{σ} and e_Y^{ρ} are direction cosines relating the axes of the pair frame to the laboratory scattering

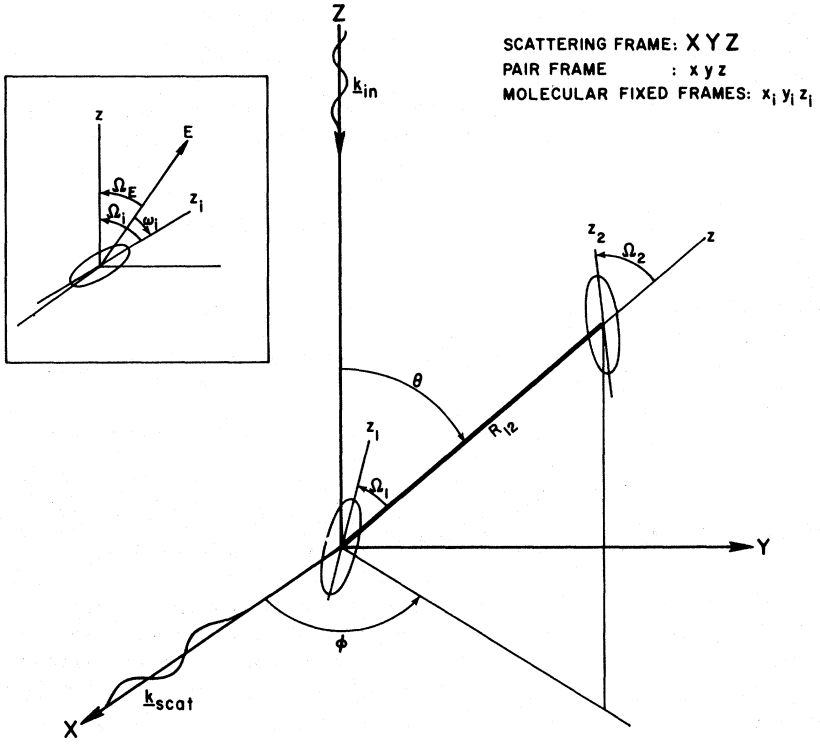

FIG. 5. Coordinate systems and angles used in calculating the scattering efficiencies.

frame and the $|m_1 m_2\rangle$ representation is given in Fig. 1. The resulting expressions are complicated angular functions and will not be given here. The absolute scattering efficiencies averaged over the 12 pair angles, Eq. (2), for various polarizations are given in Table II. Intensities for $XY+XZ$ polarization, the one used in the experiments to minimize the unshifted scattered light intensity, are given both for a single crystal oriented with the c axis parallel to Z, and for a powder average.[24] A comparison shows very little difference between the two.

In the experiment, two spectral features were observed. The theoretical relative intensity of the lower-frequency-to-higher-frequency feature for $XY+YZ$ polarization is

$$\frac{S(8,9\to4)+S(8,9\to2,3)}{S(8,9\to1)}=14, \tag{10}$$

which compares well with the experimental value of 10 ± 5.

V. FREQUENCIES

The frequencies of the observed transitions yield information both on the nature of the anisotropic intermolecular interactions and on the influence of the zero-point motion. In these quantum crystals, the large zero-point motion (of order 10% of the lattice spacing) has significant effects on the intermolecular interactions. Harris[10] first cal-

TABLE II. Raman intensities for pair transitions at various polarizations in the laboratory frame. The absolute scattering efficiencies are obtained by multiplying entries above by the factor $(80/72\pi)(\omega/c)^4 c_2\rho_0 n_i(\alpha_\parallel-\alpha_\perp)^2$. The intensities given are for single transitions and do not include an average over initial states or sum over final states. $\vec{k}_{in}$ is the propagation vector of the incident laser light.

Transition \ Polarization	Transition frequency, EQQ only	Intensities: Single crystal, $\vec{k}_{in} \parallel c$ axis					Powder
		XY	XZ	YY	YZ	$XY+XZ$	$XY+YZ$
$8\to4,\ 9\to4$	4Γ	56	64	72	64	120	$120\times24/25$
$8\to2,\ 9\to3$	5Γ	42	48	54	48	90	$90\times24/25$
$8\to1,\ 9\to1$	10Γ	7	8	9	8	15	$15\times24/25$
$7\to5,\ 7\to6$	0	21	24	27	24	45	$45\times24/25$
$4\to1$	6Γ	60	48	84	48	108	$108\times48/45$
$4\to2,\ 4\to3$	1Γ	58	56	78	56	114	$114\times288/285$
$2\to1,\ 3\to1$	5Γ	29	28	39	28	57	$57\times288/285$

culated these effects using Nosanow's wave function to represent the molecular coordinates. The variational wave function is composed of a Hartree single-particle Gaussian-type wave function ϕ modified by a short-range Jastrow correlation factor f_{jk}:

$$\psi(r_1, \ldots, r_n) = \prod_i \phi\,(|\vec{r}_i - \vec{R}_i|) \prod_{j<k} f_{jk}(r_{jk}), \qquad (11)$$

where $\vec{r}_i$ is the position of molecule i, $\vec{R}_i$ its equilibrium position, and $\vec{r}_{jk} = \vec{r}_k - \vec{r}_j$. The isotropic intermolecular interaction is taken to be the Lennard-Jones (LJ) potential V_{LJ} and the correlation and Gaussian factors are

$$f_{jk} = \exp[-KV_{LJ}(r_{jk})] \qquad (12)$$

and

$$\phi = \exp[-|r_i - R_i|^2/2\sigma^2]\,. \qquad (13)$$

The variational parameters K and σ are chosen to minimize the lattice energy. The result of averaging the EQQ interaction over this ground state is simply to renormalize the rigid lattice coupling parameter Γ_0 by a constant, i.e., $\Gamma = \xi_{54}\Gamma_0$. Using the available quantum crystal results for H_2 and a mass scaling procedure for D_2, Harris found ξ_{54} to be 0.93 for both molecules. However, the D_2 wave function subsequently calculated by Nosanow[25] does not scale from that of H_2. We have recalculated ξ_{54} using this wave function and find a value of 0.96 for D_2. Because these results looked promising for explaining our observations, it seemed important to determine the sensitivity of ξ_{54} to the choice of wave function.

A more general wave function of this type has been considered by Krumhansl and Wu[26] for solid hydrogen. They generalized the form of the correlation factor and performed numerical computations for Lennard-Jones, Buckingham exp-6, and the nonspherical Wang-Chang molecular potentials. We have used these wave functions to calculate the EQQ reduction factor ξ_{54} and find that although at low pressure the total lattice energy changes little with the choice of these wave functions, the variation of ξ_{54} is significant. Results, along with those calculated for other wave functions, are listed in Table III. We note that the observed ratio $\nu_h/10\Gamma_0$ is 0.81 for D_2 and 0.79 for H_2. However, these cannot be directly compared with ξ_{54} because of other perturbations (see Table I).

Wave functions of the form given in Eq. (11) ignore long-range correlations, and, as Noolandi and Van Kranendonk[27] have recently pointed out, these may have as large an effect on the EQQ interaction as the short-range correlations. The EQQ interaction can be renormalized for both types of correlations by using a collective wave function[28] of the form

$$\psi_c(\vec{r}_1, \ldots, \vec{r}_n) = \exp[-\tfrac{1}{2}\sum_{i\neq j} \tfrac{1}{2}\vec{u}_{ij} \cdot \overleftrightarrow{D}_{ij}^{-1} \cdot \vec{u}_{ij}] \prod_{k<l} f_{kl}(r_{kl})\,, \qquad (14)$$

where $\overleftrightarrow{D}_{ij}$ is the displacement-displacement correlation function and $\vec{u}_{ij} = \vec{r}_{ij} - \vec{R}_{ij}$. Noolandi and Van Kranendonk estimated the reduction of Γ_0 due to long-range correlations in H_2 to be ~10% by using empirical values for the components of $\overleftrightarrow{D}_{ij}$ and setting $f_{ij} = 1$. They assumed additivity of the long- and short-range contributions to ξ_{54} to find a total value of 0.80 to 0.85. We have used the self-consistent collective wave function calculated by Klein and Koehler[11] (based on an LJ potential and a one-parameter Jastrow function) to average the EQQ potential, finding ξ_{54} to be 0.68 for H_2 and 0.79 for D_2. Since this wave function not only gives the best lattice energy, but also takes into account both long- and short-range correlations, it has been used to calculate zero-point averages of all of the important interactions considered in Table I.

In addition to the perturbations of the energy levels already discussed, consideration of the linear phonon-rotation interaction has been estimated to *increase* the effective coupling Γ by ~5%.[10] As pointed out by Harris, this calculation still requires some refinement and for this reason it has not been included in the column "Resultant theor freq." of Table I. The effect of the non-EQQ interactions was also omitted from this column because the potential parameters are not reliably known and must be regarded as a subject for further experimental work. To determine these parameters, more of the transitions must be observed or resolved. Nevertheless, if our assignments are indeed correct, to within experimental accuracy no deviations from the EQQ anisotropic potential can be identified, and we must regard such effects as either small or perturbing the observed transitions in an unlikely man-

TABLE III. Theoretical values of the EQQ scaling parameter ξ_{54} for several forms of the lattice wave function.

Wave-function source potential	Krumhansl-Wu LJ	Krumhansl-Wu exp-6	Krumhansl-Wu Wang-Chang	Single particle Hartree Nosanow LJ	Klein-Koehler LJ	Collective Klein-Koehler LJ
D_2	...	...	...	0.96	0.92	0.79
H_2	0.88	0.91	0.86	0.93	0.84	0.68

ner such that they scale as Γ and cannot be distinguished from the renormalization.

VI. CONCLUSION

Direct observation of the pair spectra has provided the most complete and reliable information to date concerning the anisotropic intermolecular interactions in the solid. A point EQQ pair interaction appears to be sufficient to explain the data. Large reductions of the transition frequencies from those expected for a rigid lattice are mostly accounted for by averaging the interactions over the zero-point motion with a collective wave function. On the basis of the zero-point average alone, using what is believed to be the best available wave function, theory predicts a lower value than is observed. This can probably be accounted for by the phonon-rotation interaction which should be larger for H_2 than D_2. The sensitivity of the averaged interactions to the form of the isotropic potential and Jastrow function has been pointed out and it is hoped that the present data will motivate more refined calculations of the ground-state wave function.

ACKNOWLEDGMENTS

We thank S. P. S. Porto and L. Fraas for the generous loan of their iodine filter; M. L. Klein and T. R. Koehler, J. A. Krumhansl and S. Y. Wu, and L. H. Nosanow for providing us with their unpublished results; N. R. Werthamer and J. Van Kranendonk for useful discussions; L. Hall for programming assistance; and L. Ahlberg and J. Curnow for their technical aid.

---

*Permanent address: Natuurkundig Laboratorium, Universiteit Van Amsterdam, Amsterdam-C, Netherlands.

†Permanent address: Physics Department, University of British Columbia, Vancouver 8, B. C., Canada.

‡Contribution No. 2783 from Department of Chemistry.

[1]W. N. Hardy and J. R. Gaines, Phys. Rev. Letters 17, 1278 (1968); J. H. Constable and J. R. Gaines, Solid State Commun. 9, 155 (1971).

[2]See, for example, H. M. James, Phys. Rev. B 2, 2213 (1970), and references therein.

[3]W. N. Hardy, I. F. Silvera, and J. P. McTague, Phys. Rev. Letters 26, 127 (1971).

[4]C. F. Coll, III, A. B. Harris, and A. J. Berlinski, Phys. Rev. Letters 25, 858 (1970).

[5]H. P. Gush, W. F. J. Hare, E. J. Allin, and H. L. Welsh, Can. J. Phys. 38, 176 (1960); V. F. Sears and J. Van Kranendonk, *ibid.* 42, 980 (1964).

[6]P. A. Egelstaff, B. C. Haywood, and F. J. Webb, Proc. Phys. Soc. (London) 90, 681 (1967); R. J. Elliott and W. M. Hartmann, *ibid.* 90, 671 (1967).

[7]R. J. Roberts and J. G. Daunt, Phys. Letters 33A, 353 (1970).

[8]J. F. Jarvis, H. Meyer, and D. Ramm, Phys. Rev. 178, 1461 (1969); D. Ramm, H. Meyer, and R. L. Mills, Phys. Rev. B 1, 2763 (1970).

[9]A. B. Harris, L. I. Amstutz, H. Meyer, and S. M. Myers, Phys. Rev. 175, 603 (1968).

[10]A. B. Harris, Phys. Rev. B 1, 1881 (1970).

[11]M. L. Klein and T. R. Koehler (private communication); J. Phys. C 3, 102(L) (1970); Phys. Letters 33A, 253 (1970).

[12]T. Nakamura, Progr. Theoret. Phys. (Kyoto) 14, 135 (1955).

[13]The convention for the spherical harmonics and Clebsch-Gordan coefficients is that of M. E. Rose, *Elementary Theory of Angular Momentum* (Wiley, New York, 1957).

[14]The crystal field arising from the second term in Eq. (1) summed over nearest neighbors vanishes in a rigid ideal hcp lattice ($c/a=\sqrt{\frac{8}{3}}$) when the neighbors are identical.

[15]I. F. Silvera, W. N. Hardy, and J. P. McTague, Discussions Faraday Soc. 48, 54 (1969).

[16]L. L. Chase, J. L. Davis, G. E. Devlin, and S. Getschwind (unpublished).

[17]I. F. Silvera, W. N. Hardy, and J. P. McTague, Rev. Sci. Instr. (to be published).

[18]For a random distribution of $J=1$ molecules of mole fraction c in the hcp lattice, the mole fraction of isolated $J=1$ pairs, c_2 can be calculated from the relationship $c_2=6c^2(1-c)$[18].

[19]There is evidence that, at temperatures below 4.2 K, o-H_2 molecules tend to cluster, yielding pair concentrations greater than those calculated from a random (high-temperature) distribution. Cf. L. I. Amstutz, J. R. Thompson, and H. Meyer, Phys. Rev. Letters 21, 1175 (1968).

[20]I. F. Silvera, W. N. Hardy, and J. P. McTague (unpublished).

[21]E. B. Wilson, J. C. Decius, and P. C. Cross, *Molecular Vibrations* (McGraw-Hill, New York, 1955), p. 48.

[22]W. N. Hardy, I. F. Silvera, and J. P. McTague (unpublished).

[23]R. Loudon, Advan. Phys. 13, 432 (1964).

[24]The powder averages were obtained both from the sum rule $\sum_{\sigma,\rho}|\langle j|\alpha^P_{\sigma\rho}|i\rangle|^2=$constant, and as a check by averaging Eq. (9).

[25]L. H. Nosanow (private communication); K. N. Klump, O. Schnepp, and L. H. Nosanow, Phys. Rev. B 1, 2496 (1970).

[26]J. A. Krumhansl (private communication); J. A. Krumhansl and S. Y. Wu, Phys. Letters 28A, 263 (1968).

[27]J. Noolandi and J. Van Kranendonk, Phys. Letters 30A, 258 (1969); Can. J. Phys. 48, 675 (1970).

[28]An excellent discussion of quantum crystal wave functions is given by N. R. Werthamer, Am. J. Phys. 37, 763 (1969).